Journal of Mechanics in Medicine and Biology
Vol. 13, No. 6 (2013) 1340013 (12 pages)

DOI: 10.1142/S0219519413400137

A MATHEMATICAL MODEL FOR MICRO- AND NANO-SWIMMERS

YUAN-QING XU*, FANG-BAO TIAN*,†,‡,
XIAO-YING TANG* and YU-HUA PENG*

*School of Life Science, Beijing Institute of Technology
Beijing 100081, P. R. China

†Department of Mechanical Engineering, Vanderbilt University
2301 Vanderbilt Pl., Nashville
TN 37235-1592, USA

‡fangbao.tian@vanderbilt.edu; onetfbao@gmail.com

Received 27 June 2013
Revised 27 August 2013
Accepted 30 August 2013
Published 13 December 2013

In order to explore the kinetic characteristics of planktonic microorganisms and nanometer biological motors, a mathematical model is developed to estimate the hydrodynamic force in the migration of micro- and nano-swimmers by using the Laplace transformation and linear superposition. Based on the model, it is found that a micro- and nano-swimmer will enjoy a positive propulsive force by improving frequencies or generating traveling waves along its body if it is not time reversible. The results obtained in this study provide a physical insight into the behaviors of the micro- and nano-swimmer at low Reynolds numbers, and the corresponding quantitative basis can also be potentially used in the design of nanorobot and nanosized biomaterials.

Keywords: Mathematical model; micro- and nano-swimmers; nanosized; biomaterials.

1991 Mathematics Subject Classification: 22E46, 53C35, 57S20

1. Introduction

In the micro/nano scale, an ultra micro-swimmer such as bacteria, flagellated nanorobot and molecular motor etc experiences an environment quite different from that with big size and high velocity in low viscosity fluid.[1,2] Specifically, because of their small size (of the order of micro/nano meters) and the low velocity (of the order of micro/nano meters per second), the Reynolds number, defined by their size and velocity of them, is much less than 1, and hence, the fluid inertia is essentially irrelevant to them.[1,3] Childress[4] showed that a neutrally buoyant

‡Corresponding author.

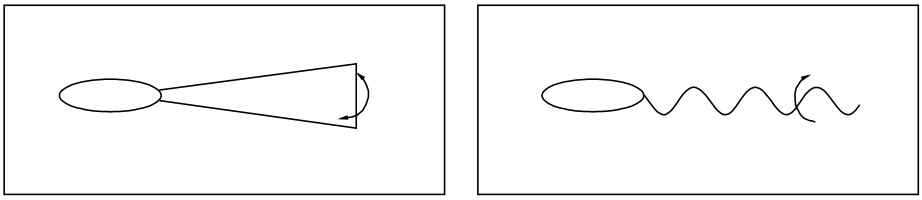

(a) (b)

Fig. 1. Two types of bio-locomotion: (a) Flapping fin propulsion of large aquatic animal; (b) traveling helical wave propulsion of a micro- or nano-swimmer.

organism exhibiting time-reversal symmetry is a non-swimmer in the Stokesian realm. More recently, Lowe[5] argued that the irrelevant-inertia for microorganisms makes it difficult for them to move. Therefore, the microorganisms must improve their frequencies (so as to make $\sigma\text{Re} = \omega L^2/\nu = O(1)$) or perform a new propulsive method other than flapping fin (see Fig. 1(a)) to break the time-reversal symmetry to swim, such as by traveling helical wave down the filament (see Fig. 1(b)).[4,6]

In the last few decades, there has been considerable interest in understanding the dynamics of animal swimming. Numerical approaches, such as the finite element method,[6,7] the immersed boundary — finite difference method,[8–12] and the immersed boundary — lattice Boltzmann method,[13–20] have been applied to simulate the animal swimming. Taylor,[21,22] Hancock,[23] Lighthill[24] and Wu[25] studied the microorganism swimming by solving the Stokes and Navier–Stokes equations under the assumptions of very low viscosity of water, plane wave propagating, negligible inertial forces and small amplitude of the waves. Machin[26] showed a theoretical approach by considering the types of wave propagation which may occur along an elastic filament immersed in a viscous medium. A semi-empirical approach was introduced by Azuma.[27] Some experimental and theoretical models are also found in the works of Kim *et al.*,[28] Srigiriraju and Powers,[29] Avron *et al.*[30] and Yu *et al.*[31] Elasticity or semi-elasticity theory was employed in this realm and numbers of high quality works were reported by Wiggins and Goldstein,[32] Camalet *et al.*,[33] Wolgemuth *et al.*[34] and Powers.[35] But few studies tried to work on the analytical solution of linearized Navier–Stokes equations in this realm.

The exact solutions to the flow field and hydrodynamic force on a micro- or nano-swimmer performing traveling wave down along the filament or rigid flap are presented in the present work. Assuming that the amplitude of the traveling wave or flap is small, Navier–Stokes equations are linearized by ignoring the convective term. The linearized equation can be transformed to the form that just contains spacial variables, by using the Laplace transformation. Thus, the eigenvalues and eigenfunctions of this equation can be obtained and then the solution of the reduced Navier–Stokes equations on the half plane with surface executing traveling wave or rigid flap of arbitrary frequency can be derived by employing the principle of linear superposition based on these eigenfunctions.

Consequently, the other information of the flow field and hydrodynamic force on the micro- or nano-swimmer is obtained. The numerical results indicate that our model can simulate the micro/nano swimming principle effectively, it also can be potentially used for the design of nanorobot and molecular motor which are driven by a flagellum in the fluid.

2. Problem Formulation and Theory

As shown schematically in Fig. 2, a micro- or nano-swimmer immersed in low viscous and quiescent fluid undergoing a traveling wave motion or rigid flap is considered. The fluid motion is governed by the incompressible Navier–Stokes equations.

$$\nabla \cdot \mathbf{u} = 0, \tag{1}$$

$$\rho\left(\frac{\partial \mathbf{u}}{\partial t} + \mathbf{u} \cdot \nabla \mathbf{u}\right) = -\nabla p + \mu \nabla^2 \mathbf{u}, \tag{2}$$

where $\mathbf{u}$ is the velocity, p is the pressure, ρ and μ are the density and viscosity of the fluid, respectively. Assuming that the amplitude of the traveling wave or flap is much smaller than the characteristic scale of the flow (the length of the micro- or nano-swimmer especially) and μ is very high so that the Reynolds number is low, the nonlinear term in Eq. (2) is ignored and the incompressible Navier–Stokes equations can be rewritten as

$$\nabla \cdot \mathbf{u} = 0, \tag{3}$$

$$\rho \frac{\partial \mathbf{u}}{\partial t} = -\nabla p + \mu \nabla^2 \mathbf{u}. \tag{4}$$

Therefore, the principle of linear superposition can be applied to the simplified system. The boundary conditions are described as follows

$$\mathbf{u}|_s = \mathbf{f}(\mathbf{r}(s), t), \tag{5}$$

$$\mathbf{u}|_\infty = 0, \tag{6}$$

where s is the arc length of the micro- or nano-swimmer, which is approximately equal to x considering the small amplitude assumption.

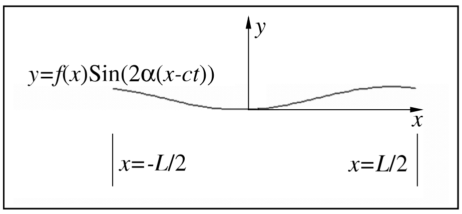

Fig. 2. Sketch of the physical problem.

For any motion of the micro- or nano-swimmer, it can be described as $y = g(x,t)$. Under the small amplitude assumption, y can be expanded as

$$y = \sum_{m=0,n=0}^{\infty} a_{mn} x^m \sin[w_n(t + t_n)], \tag{7}$$

where $a_{mn} x^m \sin[w_n(t + t_n)]$ $(m, n \in \mathbf{N})$ is the basic movement of the micro- or nano-swimmer.

The movement of the micro- or nano-swimmer and the flow field before $t = t_0$ are not important for us. From Eq. (7), two characteristics of the movement are drawn: (1) the micro- or nano-swimmer keeps still before $t < t_0$ and the movement starts when $t \geq t_0$ (we take $t_0 = 0$ for simplicity in this article); (2) the basic movement is to be oscillating periodically. It is convenient to introduce the Laplace transformation before solving the Eqs. (3)–(6). The Laplace transformation of $f(t)$ is denoted as $F(s) = L[f(t)]$, which is defined as[36]

$$F(s) = \int_0^{\infty} f(t) e^{-st} dt. \tag{8}$$

If there exists a real constant t_0 and A such that $|f(t)| < Ae^{\alpha t} : t > t_0$, we may say that $f(t)$ is of exponential order α. Similarly, if $\int_0^{t_0} f(t)dt$ exists and $f(t)$ is of exponential order α, then the Laplace transform $F(s)$ exists for $\mathrm{Re}[s] > \alpha$.[36]

The inverse Laplace transformation is denoted as $f(t) = L^{-1}[F(s)]$ and defined as

$$f(t) = \frac{1}{2\pi i} \int_{\alpha - i\infty}^{\alpha + i\infty} F(s) e^{st} ds, \tag{9}$$

where α is a real constant to the right of all singularities of $F(s)$, namely, there is no singularity of $F(s)$ except $\mathrm{Re}(s) \leq \alpha$. Equation (9) is calculated by employing the theory of residues[36]

$$f(t) = \sum_{k=1}^{n} \mathrm{Res}[F(s)e^{st}, s_k], \tag{10}$$

where $s_1, s_2, \ldots, s_n$ are the poles of $F(s)$, which is analytic except for these poles.

From physical view, the velocity and pressure of the fluid field are of exponential order 0. Thus from the analysis above, the Laplace transformations of velocity and pressure of the fluid field exists when $\mathrm{Re}[s] > 0$. Using the Laplace transformation, the transformed control equations are obtained

$$\nabla \cdot \mathbf{U} = 0, \tag{11}$$

$$s\rho\mathbf{U} - \rho\mathbf{u}|_{t=0+} = -\nabla P + \mu\nabla^2\mathbf{U}, \tag{12}$$

where $s = \alpha - iq$ with $\alpha \to 0$ and $\alpha > 0$, namely, for any $\varepsilon > 0$, $\varepsilon > \alpha > 0$. The initial velocity $\mathbf{u}|_{t=0^+}$ is taken to be zero because the influence of the boundary condition has not diffused into the field yet.

Taking the curl of the momentum equation (Eq. (12)) twice and using the incompressible condition, we obtain

$$\nabla^2\left(\nabla^2\mathbf{U} - \frac{s}{\nu}\mathbf{U}\right) = 0, \tag{13}$$

where ν is the kinematic viscosity of the fluid ($\nu = \mu/\rho$).

Because the surface is executing normal harmonic motion, the velocity field can be expanded as

$$\mathbf{U}(x, y|s) = \mathbf{U}_s(y|s)e^{imx}, \tag{14}$$

where $i = \sqrt{-1}$. Substituting Eq. (14) into Eq. (13), we get

$$\frac{\partial^4\mathbf{U}_s}{\partial y^4} - \left(2m^2 + \frac{s}{\nu}\right)\frac{\partial^2\mathbf{U}_s}{\partial y^2} + \left(m^4 + \frac{s}{\nu}m^2\right)\mathbf{U}_s = 0. \tag{15}$$

The eigenvalues of Eq. (15) are $-\sqrt{m^2}$ and $-\sqrt{m^2 + s/\nu}$ for the upper half plane $y \geq 0$, and $\sqrt{m^2}$ and $\sqrt{m^2 + s/\nu}$ for the other plane $y \leq 0$. Here we just consider the upper half plane because of the symmetry of V and the antisymmetry of U and P about $y = 0$, the last leads to $P|_{y=0} = 0$ at $|x| > L/2$. The flow field is the linear combination of the eigenfunctions $e^{-\sqrt{m^2}y}$ and $e^{-\sqrt{m^2+s/\nu}y}$, as

$$U_s(y|s) = isy_0\frac{m\sqrt{m^2 + \frac{s}{\nu}}}{\sqrt{m^2}(\sqrt{m^2} - \sqrt{m^2 + \frac{s}{\nu}})}(e^{-\sqrt{m^2}y} - e^{-\sqrt{m^2+\frac{s}{\nu}}y}), \tag{16}$$

$$V_s(y|s) = \frac{-sy_0}{\sqrt{m^2} - \sqrt{m^2 + \frac{s}{\nu}}}\left(\sqrt{m^2 + \frac{s}{\nu}}e^{-\sqrt{m^2}y} - \sqrt{m^2}e^{-\sqrt{m^2+\frac{s}{\nu}}y}\right), \tag{17}$$

and

$$U(x, y|s) = isy_0\frac{m\sqrt{m^2 + \frac{s}{\nu}}}{\sqrt{m^2}(\sqrt{m^2} - \sqrt{m^2 + \frac{s}{\nu}})}e^{imx}(e^{-\sqrt{m^2}y} - e^{-\sqrt{m^2+\frac{s}{\nu}}y}), \tag{18}$$

$$V(x, y|s) = \frac{-sy_0}{\sqrt{m^2} - \sqrt{m^2 + \frac{s}{\nu}}}e^{imx}\left(\sqrt{m^2 + \frac{s}{\nu}}e^{-\sqrt{m^2}y} - \sqrt{m^2}e^{-\sqrt{m^2+\frac{s}{\nu}}y}\right), \tag{19}$$

$$P(x, y|s) = -\frac{\rho s^2 y_0\sqrt{m^2 + \frac{s}{\nu}}}{\sqrt{m^2}(\sqrt{m^2 + \frac{s}{\nu}} - \sqrt{m^2})}e^{-\sqrt{m^2}y}e^{imx}. \tag{20}$$

The transformed boundary conditions are

$$y = y_0x^m: \quad m \in N, \ |x| \leq L/2, \tag{21}$$

$$v(x, 0|s) = sy_0x^m: \quad m \in N, \ |x| \leq L/2, \tag{22}$$

$$p(x, 0|s) = 0: \quad |x| > L/2, \tag{23}$$

where $y_0 = ae^{st_n}\omega_n/(s^2 + \omega_n^2)$.

The solution of the linear Navier–Stokes equations can be deduced using the boundary conditions given by Eqs. (22) and (23). We normalize the equations by $\hat{x} = x/L$, $\hat{y} = y/L$, $\mathrm{Re} = \rho s L^2/\mu$ and $\kappa = mL$. It should be pointed out that the definition of Re in the present work is different from that in Ref. 37. In the present work, Re is a complex number with an infinitesimal real part while it is a real number in Ref. 37. Inspired by the work of Van Eysden and Sader,[37] we will discuss the conditions of m being an odd and even number.

First situation that m is odd is discussed. The boundary condition can be described as follows

$$\int_0^\infty \chi(\kappa, \mathrm{Re})\sqrt{\kappa^2}\left(1 - \frac{\sqrt{\kappa^2}}{\sqrt{\kappa^2 + \mathrm{Re}}}\right)\sin\kappa\hat{x}\,d\kappa = \hat{x}^{2n+1}: \quad n \in N, \ |\hat{x}| \le 1/2, \tag{24}$$

$$\int_0^\infty \chi(\kappa, \mathrm{Re})\sin\kappa\hat{x}\,d\kappa = 0: \quad |\hat{x}| > 1/2. \tag{25}$$

From the book by Lavrent'ev and Shabat,[38] we have the following relation

$$\int_0^\infty J_{2n-1}(t/2)\sin(tx)dt$$
$$= \begin{cases} \mathrm{Im}\left[\dfrac{(1/2)^{2n-1}}{\sqrt{1/4 - x^2}(\sqrt{1/4 - x^2} + ix)^{2n-1}}\right]: & |x| < 1/2, \\ F(x, n)\sin(n\pi): & |x| > 1/2, \end{cases}$$

where $n \in Z$. It is expected that the pressure contains a square root singularly near the edges of the micro- or nano-swimmer at $|\hat{y}| = 1/2$. Using the principle of superposition, χ is obtained

$$\chi(\kappa, \mathrm{Re}) = \sum_{m=1}^{M} a_m J_{2m-1}(\kappa/2). \tag{26}$$

The $\sin(\kappa\hat{x})$ can be expanded into a series around $\hat{x} = 0$, which is given as

$$\sin(\kappa\hat{x}) = \sum_{n=0}^{\infty} \frac{(-1)^n}{(2n+1)!}(\kappa\hat{x})^{2n+1}. \tag{27}$$

Substituting Eqs. (26) and (27) into Eq. (24) and using the result of Eq. (25), we get

$$\sum_{m=1}^{M} A_{q,m} a_m = \begin{cases} \dfrac{(2n-1)!}{(-1)^{n-1}}: & q = n, \\ 0: & q \ne n, \end{cases} \tag{28}$$

where

$$A_{q,m} = \int_0^\infty \kappa^{2q-1}\sqrt{\kappa^2}\left(1 - \frac{\sqrt{\kappa^2}}{\sqrt{\kappa^2 + \mathrm{Re}}}\right)J_{2m-1}(\kappa/2)d\kappa.$$

The stress tensor of the Newton fluid field is $\sigma_{ij} = -p\delta_{ij} + \mu(u_{i,j} + u_{j,i})$ $(i, j = 1, 2;$ $\delta_{ij} = 1$ if $i = j$, else $\delta_{ij} = 0$; 1 denotes x-direction, 2 denotes y-direction). For the small amplitude motion, the micro- nano-swimmer normal $\mathbf{n} = \mathbf{k} \times d\mathbf{r}/ds \simeq (0, 1)$, where $\mathbf{k}$ is the unit vector perpendicular to $x - y$ plane. Then the force acting on the upper surface of the filament is $f_j = -p\delta_{2j} + \mu(u_{2,j} + u_{j,2})$. For $j = 1$, $f_1|_s = \mu(u_{2,1} + u_{1,2})|_{y=0}$. Considering that u_1 and u_2 are antisymmetric and symmetric about $y = 0$, respectively, $u_{1,2}$ and $u_{2,1}$ are both symmetric about $y = 0$. Thus, the x-direction of the force acting on per unit length of the filament is zero. For $j = 2$, the $u_{2,2}|_s$ is zero from Eq. (19) and $f_2|_s = -p|_{y=0}$. The hydrodynamic force in the z-direction per unit length is

$$\begin{aligned} \Delta P &= P(\hat{x}, 0^-|s) - P(\hat{x}, 0^+|s) \\ &= -\rho s^2 L y_0 \sum_{m=1}^{M} 2a_m \int_0^\infty J_{2m-1}(\kappa/2) \sin(\kappa\hat{x}) d\kappa \\ &= -\rho s^2 L y_0 \sum_{m=1}^{M} \frac{8a_m \hat{x}}{\sqrt{1-4\hat{x}^2}} U_{2m-1}(\sqrt{1-4\hat{x}^2}), \end{aligned} \tag{29}$$

where U_{2m-1} are the Chebyshev polynomials of the second kind of order $2m - 1$.

Now we consider the situation in which m is even. The boundary condition can be rewritten analogous to that of odd m

$$\int_0^\infty \chi(\kappa, \mathrm{Re})\sqrt{\kappa^2}\left(1 - \frac{\sqrt{\kappa^2}}{\sqrt{\kappa^2 + \mathrm{Re}}}\right) \cos \kappa\hat{x} d\kappa = \hat{x}^{2n}: \quad n \in N, \ |\hat{x}| \le 1/2, \tag{30}$$

$$\int_0^\infty \chi(\kappa, \mathrm{Re}) \cos \kappa\hat{x} d\kappa = 0: \quad |\hat{x}| > 1/2. \tag{31}$$

Also, we can get the analogous result from the book of Lavrent'ev and Shabat[38] we get$(n\epsilon Z)$

$$\int_0^\infty J_{2n}(t/2)\cos(tx)dt = \begin{cases} \mathrm{Re}\left[\dfrac{(1/2)^{2n}}{\sqrt{1/4 - x^2}(\sqrt{1/4 - x^2} + ix)^{2n}}\right]: & |x| < 1/2, \\ F(x, n)\sin(n\pi): & |x| > 1/2. \end{cases}$$

Using the similar process, we get

$$\chi(\kappa, \mathrm{Re}) = \sum_{m=1}^{M} a_m J_{2m}(\kappa/2), \tag{32}$$

$$\sum_{m=1}^{M} A_{q,m} a_m = \begin{cases} \dfrac{(2n-2)!}{(-1)^{n-1}}: & q = n, \\ 0: & q \neq n, \end{cases} \tag{33}$$

where

$$A_{q,m} = \int_0^\infty \kappa^{2q-2}\sqrt{\kappa^2}\left(1 - \frac{\sqrt{\kappa^2}}{\sqrt{\kappa^2 + \mathrm{Re}}}\right) J_{2m-2}(\kappa/2) d\kappa$$

and

$$\Delta P = P(\hat{x}, 0^-|s) - P(\hat{x}, 0^+|s)$$
$$= -\rho s^2 L y_0 \sum_{m=1}^{M} \frac{4a_m}{\sqrt{1-4\hat{x}^2}} T_{2m-2}(\sqrt{1-4\hat{x}^2}), \tag{34}$$

where T_{2m-2} is the Chebyshev polynomials of the first kind of order $2m-2$.

The coefficient $a_m(0 \geq m \leq M)$ calculated from Eqs. (28) and (33) is substituted into Eqs. (26) and (32), then $\chi(\kappa, \mathrm{Re})$ is obtained.

Comparing the present method with that in Ref. 37, it is found that the present work utilizes the Laplace transformation rather than the Fourier transformation used in Ref. 37. This is because we are just interested in the flow field and hydrodynamical characteristics when $t \geq t_0$, while long time occurred motion is required in the Fourier transformation in Ref. 37. The results are consistent with that in the Ref. 37 by using "$-i\omega$" to displace "s", which can be taken as a validation of the present method.

To further validate the present result, we take the curl of the momentum equation once and obtain

$$s\mathbf{W} = \nu\nabla^2\mathbf{W}, \tag{35}$$

where $\mathbf{W}$ is the Laplace transformation of the vorticity $\mathbf{w}$. It is easy to get the general solution of this equation

$$W_z = Ae^{-\sqrt{m^2+s/\nu}y}e^{imx}. \tag{36}$$

Taking the curl of the velocity in Eqs. (18) and (19), the vorticity also can be obtained

$$W_z' = \frac{is^2 y_0}{\nu(\sqrt{m^2} - \sqrt{m^2+s/\nu})} e^{-\sqrt{m^2+s/\nu}y}e^{imx}. \tag{37}$$

W_z' derived from $\nabla \times \mathbf{U}$ is the same as W_z derived from the vorticity dynamic equation. This fact further validates the method in the present work.

3. Two Applications: Traveling Wave and Rigid Flap

We have emphasized several times that the amplitude of motion is small enough so that the boundary condition and the Navier–Stokes equations can be linearized, and the principle of linear superposition can be applied. Here, two applications, including traveling wave and rigid flap, are discussed.

3.1. *Traveling wave*

A traveling wave with constant amplitude, described as $\hat{y} = a_0 \sin[\omega(\hat{x} - ct)]$, is considered. In order to make the problem simpler, the parameters ω and c are taken as $\omega = 2\pi$ and $c = 1$, respectively. The traveling wave can be expanded as the superposition of basic motions.

$$\begin{aligned}\hat{y} &= a_0 \sin[2\pi(\hat{x} - t)] \\ &= a_0[\cos(2\pi\hat{x})\sin(2\pi t_1) + \sin(2\pi\hat{x})\sin(2\pi t_0)],\end{aligned} \tag{38}$$

where $t_0 = t + 1/4$ and $t_1 = t + 1/2$. The trigonometric functions $\sin(2\pi x)$ and cos $(2\pi x)$ are expanded around $\hat{x} = 0$ as

$$\sin(2\pi\hat{x}) = \sum_{n=0}^{\infty} \frac{(-1)^n}{(2n+1)!}(2\pi\hat{x})^{2n+1},$$

$$\cos(2\pi\hat{x}) = \sum_{n=0}^{\infty} \frac{(-1)^n}{(2n)!}(2\pi\hat{x})^{2n}.$$

It is sufficient to take the first six terms of the series, M in Eqs. (28) and (33) is 12. Taking the integral of the hydrodynamic force along the micro- nano-swimmer and using the inverse Laplace transformation, we get the whole force acting on it, as shown in Fig. 3. We find that it is periodic except at the time $t = 0$, where the force is infinity, because the motion occurs at this time suddenly and the acceleration at the boundary is infinity. The amplitude of side force (C_L) is much lager than that of thrust (C_D) and the average C_L is zero. The average C_D is less than zero, which means that the micro- nano-swimmer performing this type of motion could generate an efficient thrust to push it forward.

3.2. *Rigid flap*

A pitching and plunging rigid plate (as a special model of micro- or nano-swimmer) in flow is considered. The motion of the plate can be described as $\hat{y} = a_0 \sin(\omega t) + \theta_0 \hat{x} \sin(\omega t + 1/2\pi)$. In order to make the problem simpler, we take $\omega = 2\pi$ and

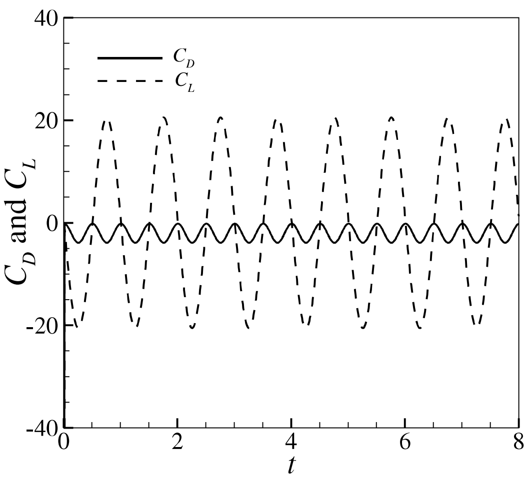

Fig. 3. C_D and C_L for the traveling wave case.

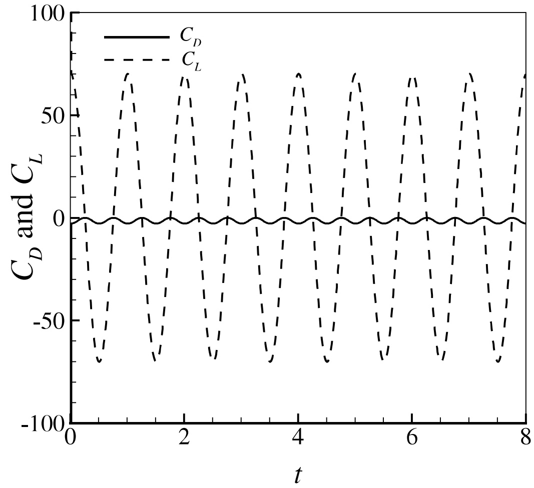

Fig. 4. C_D and C_L for the rigid flap case.

$\theta_0 = a_0$. Thus, the motion is rewritten as

$$\hat{y} = a_0\{\sin(2\pi t) + \hat{x}\sin[2\pi(t + 1/4)]\}. \tag{39}$$

Then a similar process as Sec. 3.1 is performed and the C_D and C_L of the plate are obtained, as shown in Fig. 4. It is found that a very small thrust can be generated in this type of motion and it is in contrast with that derived from the Stokes equations which ignore all the inertia terms. In the Stokes flow regime, a swimmer performing flap motion cannot generate thrust.[1]

It is obvious that the thrust of the plate is proportional to the amplitude and frequency of the flap. The frequency reveals the unsteady characteristics of the motion and can be any real value. If the frequency is small, the thrust on the plate is very small and the swimming distance is microscopic. It is found that the micro- or nano-swimmer may go ahead several percents of its body length after hundreds or thousands of years. In this sense, it is regarded that the micro- or nano-swimmer at low Reynolds number with rigid flap motion is the same as that in the Stokes flow. In contrast, if the frequency is large and the corresponding thrust is larger, we can see a considerable swimming distance of the micro- or nano-swimmer in several minutes.

4. Conclusions

The Laplace transformation and the principle of linear superposition based on eigenfunctions are used to solve the linearized Navier–Stokes equations analytically. The solutions are applied on two types of motion, traveling wave and rigid flap. The results show that the micro- or nano-swimmer can swim forward at low Reyholds numbers by improving their frequencies or performing the traveling wave down along its body. This study presents a mathematical model, which can direct the behaviors of the micro- and nano-swimmers at low Reynolds numbers. The model is significant for the understanding of motion of the nanorobot and molecular motor which are driven by a flagellum in a fluid, it is also an efficient analysis model for the design of artificial nanosized biomaterial for directional transport in the micro/nano scale, such as the drug transport.

Acknowledgments

This work is supported by the National Science Foundation of China (No. 81301291) and the National Natural Science Foundation of China (No. 81271568).

References

1. Purcell EM, Life at low Reynolds number, *Am J Phys* **45**:3–11, 1977.
2. Deng HB, Xu YQ, Chen DD, Dai H, Wu J, Tian FB, On numerical modeling of animal swimming and flight, **52**:1221–1242, 2013.
3. Shapere A, Wilczek F, Self-propusion at low Reynolds number, *Phys Rev Lett* **58**:2051–2054, 1999.
4. Childress S, *Mechanics of Swimming and Flying*, Cambridge University Press, 1981.
5. Lowe CP, Dynamics of filaments: Modelling the dynamics of driven microfilaments, *Phil Trans R Soc Lond B* **358**:1543–1550, 2003.
6. Tian FB, Lu XY, Luo H, Propulsive performance of a body with a traveling wave surface, *Phys Rev E* **86**:016304, 2012.
7. Wang SY, Tian FB, Jia LB, Lu XY, Yin XZ, The secondary vortex street in the wake of two tandem circular cylinders at low Reynolds number, *Phys Rev E* **81**:036305, 2010.
8. Tian FB, Lu XY, Luo H, Onset of instability of a flag in uniform flow, *Theor Appl Mech Lett* **2**:022005, 2012.
9. Tian FB, Luo H, Song J, Lu XY, Force production and asymmetric deformation of a flexible flapping wing in forward flight, *J Fluids Struct* **36**:149–161, 2013.
10. Tian FB, Dai H, Luo H, Doyle JF, Rousseau B, Fluid–structure interaction involving large deformations: 3D simulations and applications to biological systems, *J Comput Phys*, in press, doi:10.1016/j.jcp.2013.10.047.
11. Tian FB, Chang S, Luo H, Rousseau B, A 3D numerical simulation of wave propagation on the vocal fold surface, *Proc 10th Int Conf Advances in Quantitative Laryngology, Voice and Speech Research*, Cincinnati, Ohio, p. 94921483, 2013.
12. Tian FB, Dai H, Luo H, Doyle JF, Rousseau B, Computational fluid-structure interaction for biological and biomedical flows, *Proc ASME 2013 Fluids Eng Division Summer Meeting*, Incline Village, Nevada, p. 16408, 2013.
13. Tian FB, Luo H, Zhu L, Lu XY, Interaction between a flexible filament and a downstream rigid body, *Phys Rev E* **82**:026301, 2010.
14. Tian FB, Luo H, Zhu L, Liao JC, Lu XY, An immersed boundary-lattice Boltzmann method for elastic boundaries with mass, *J Comput Phys* **230**:7266–7283, 2011.
15. Tian FB, Luo H, Lu XY, Coupling modes of three filaments in side-by-side arrangement, *Phys Fluids* **23**:111903, 2011.
16. Tian FB, Role of mass on the stability of flag/flags in uniform flow, *Appl Phys Lett* **103**:034101, 2013.
17. Xu YQ, Tian FB, Li HJ, Deng YL, Red blood cell partitioning and blood flux redistribution in microvascular bifurcation, *Theor Appl Mech Lett* **2**:024001, 2012.

18. Xu YQ, Tang XY, Tian FB, Peng YH, Xu Y, Zeng YJ, IB–LBM simulation of the haemocyte dynamics in a stenotic capillary, doi:101080/102558422012729581.
19. Xu YQ, Tian FB, Deng YL, An efficient red blood cell model in the frame of IB–LBM and its application, *Int J Biomath* **6**:1250061, 2013.
20. Zu WH, Zhang JH, Chen DD, Xu YQ, Wei Q, Tian FB, Immersed boundary-lattice boltzmann method for biological and biomedical flows, *25th Parallel Comput Fluid Dyn Conf (ParCFD2013)*, Changsha, Hunan, China, 2013.
21. Taylor GI, Analysis of the swimming of microscopic organisms, *Proc Roy Soc A* **209**:447–461, 1951.
22. Taylor GI, The action of waving cylindrical tails in propelling microscopic organisms, *Proc Roy Soc A* **211**:225–239, 1952.
23. Hancock GJ, Self-propulsion of microscopic organisms through liquids, *Proc Roy Soc Biol* **217**:96–121, 1953.
24. Lighthill J, Mathematical Biofluid dynamics, Philadelphia, *Soc Indus Appl Math SIAM*, 1975.
25. Brennen C, Winet H, Fluid mechanics of propulsion by cilia and flagella, *Annu Rev Fluid Mech* **9**:339–398, 1977.
26. Machin KE, Wave propagation along flagella, *J Exp Biol* **35**, 796–806, 1958.
27. Azuma A, *The Biokinetics of Flying and Swimming* (2nd edn.), American Institute of Aeronautics and Astronautics, Inc., Reston, 2006.
28. Kim M, Bird JC, Parys AJV, Breuer KS, Powers TR, A macroscopic scale model of bacterial flagellar bundling, *Proc Natl Acad Sci USA* **100**:15481–15485, 2003.
29. Srigiriraju SV, Powers TR, Model for polymorphic transitions in bacterial flagella, *Phys Rev E* **73**:011902, 2006.
30. Avron JE, Kenneth O, Oaknin DH, Pushmepullyou: An efficient micro-swimmer, *New J Phys* **7**:234–242, 2005.
31. Yu TS, Lauga E, Hosoi AE, Experimental investigations of elastic tail propulsion at low Reynolds number, *Phys Fluids* **18**:091701, 2006.
32. Wiggins CH, Goldstein RE, Small amplitude oscillations of a flexible thin blade in a viscous fluid: Exact analytical solution, *Phys Rev Lett* **80**:3879–3882, 1998.
33. Camalet S, Julicher F, Prost J, Self-organized beating and swimming of internally driven filaments, *Phys Rev Lett* **82**:1590–1593, 1999.
34. Wolgemuth CW, Powers TR, Goldste RE, Twirling and whirling: Viscous instabilities of rotating elastica, *Phys Rev Lett* **84**:1623, 2000.
35. Powers TR, Role of body rotation in bacterial flagellar bundling, *Phys Rev E* **65**:040903, 2002.
36. Mauch S, *Introduction to Methods of Applied Mathematics or Advanced Mathematical Methods for Scientists and Engineers*, California Institue of Technology, California, USA, 2004.
37. van Eysden CA, Sader JE, Small amplitude oscillations of a flexible thin blade in a viscous fluid: Exact analytical solution, *Phys Fluids* **18**:123102, 2006.
38. Lavrent'ev MA, Shabat BV, Methods of theory of functions of complex variables, *Uspekhi Mat Nauk* **15**(5):236–239, 1960.